ACCEPTED MANUSCRIPT available at
https://www.sciencedirect.com/science/article/pii/S0920379617307986?via%3Dihub
https://doi.org/10.1016/j.fusengdes.2017.08.021

Shutdown dose rate assessment with the Advanced D1S method for the European DCLL DEMO

Iole Palermo[1], Rosaria Villari[2], Angel Ibarra[1]

[1]CIEMAT, Fusion Technology Division, Avda. Complutense 40, 28040-Madrid, SPAIN, *iole.palermo@ciemat.es
[2]ENEA, Fusion and Technology for Nuclear Safety and Security Department, ENEA C. R. Frascati, via E. Fermi 45, 00044 Frascati (Roma), Italy

The present paper is devoted to the shutdown dose rate assessment, one of the most important safety issues in fusion power plant design and operation. The characterization of the radiation environment after the shutdown is fundamental to plan safe operation and maintenance in a fusion machine in order to guarantee the dose limits are not exceeded. In this paper the shutdown dose due to the radionuclides generated by neutron activation of reactor components have been assessed for the design of the European DCLL v3.0 developed during 2016 integrated into the generic DEMO baseline 2015 fusion reactor. The shutdown dose rate calculations from 1 day to 1 year after shutdown have been performed through the Advanced D1S method coupling the particle transport MCNP5 and ACAB inventory codes. 3D maps of shutdown dose rates, decay fluxes for the whole reactor and decay gamma heating for Eurofer structures have been provided as well as specific values at relevant positions. Results are presented and discussed also in terms of the different nuclides contributions from the various activated components. Two different divertor compositions have been also used demonstrating the importance of this component not only locally but in the global radiation field inside the plasma chamber.

1. Introduction

The assessment of the radiation environment in a fusion machine like the future demonstrative reactor DEMO is essential to demonstrate a safe and economically viable operation of such machines.

The radiation field and nuclear loads during operations are typically calculated by the use of standard particle transport codes. Besides the loads during the reactor operation, neutrons generated from the deuterium–tritium (DT) reaction inside the plasma cause significant activation of the surrounding structures which radioactive products continue to decay also after the shutdown of the machine. Hence, the gamma field generated by the decay of the radioactive nuclides needs to be characterized after the shutdown in areas where personnel access could be required for operations and maintenance purposes.

Over the past decade, two different methodological approaches have been developed in the frame of the fusion technology for the three-dimensional calculation of the shutdown dose rate: the Rigorous two-step (R2S)[1] and the Direct one-step method (D1S)[2][3]. Both tools, although with different approaches, are based on the combined use of radiation transport and inventory codes.

Advanced D1S [4][5] is a D1S tool recently developed by ENEA based on MCNP5 Monte Carlo code [6] and FISPACT [7] inventory code with novel unique features. In this work the calculations have been performed by implementing an Advanced D1S version based on the use of use of ACAB inventory code [8] instead of FISPACT.

The study has been performed for a Dual-Coolant Lithium Lead (DCLL) Breeding Blanket (BB) model [9], one of the 4 BB options conceived for the future European DEMO reactor. The procedure (model, material compositions, irradiation scenario, correction factors calculation, codes and recommendations) applied for the execution of the activity is described in Section 2. The results of the analyses after the shutdown are detailed in Section 3.

2. Methodology, assumptions and input data

2.1 Advanced-D1S method

Original Direct 1-Step method (D1S) was developed by ENEA and ITER team more than fifteen years ago for fast 3D calculations of the shutdown dose rates in fusion devices [2][3]. It is based on the use of a modified version of the MCNP5 Monte Carlo code with specially prepared nuclear cross-section data. In this approach the decay gammas of the radioactive nuclides are emitted as prompt and thus, the neutron and decay gamma, treated as prompt, are transported in a single MCNP run. Time correction factors, calculated with a proper activation code, are applied to the scored quantities to take into account the build-up and the decay of the radionuclides considered. The "Advanced-D1S" [4][5] is an improved version of D1S in which new computation capabilities have been introduced, such as the dose rate spatial mesh maps

author's email: iole.palermo@ciemat.es

and cooling time dependence. Time correction factors take into account the production and decay of each radionuclide. For mesh tally maps they are internally applied to each generated photon according to its parent and multiplied by the corresponding flux-to-dose conversion coefficient to provide directly, as an output result, the dose rate in Sv/h [5].

2.2 Application to the DCLL DEMO design analyses

The DEMO baseline 2015 design [10] consists of 18 sectors each one of 20◦ and equipped with six main components: blanket modules, divertor, back supporting structure (BSS), vacuum vessel (VV), ports (Upper, Lower and Equatorial) for maintenance procedures and toroidal field (TF) coil. In the present application, an MCNP 10◦ half sector [11] of the 360º torus tokamak has been used with reflective boundary conditions on the lateral sides to take into account full 3D transport.

Blanket modules and back supporting structure are modelled in detail using MCAM CAD-to-MCNP software [12] with separated regions for its different components according to the specific design of the DCLL concept.

The development of a DCLL BB among the EUROfusion Programme to be integrated inside the common DEMO generic reactor is currently lead by CIEMAT [13]. The DCLL concept is basically characterized by the use of self-cooled breeding zones with the liquid metal PbLi serving as tritium breeder, neutron multiplier and coolant and the ferritic–martensitic steel Eurofer-97 as structural material. In Figure 1 the neutronic model of the DEMO reactor with integrated DCLL blankets (a); its plotting in MCNP5 (b); the specific BSS and BB modules' segmentation inside a sector (c); and the main structures inside the equatorial outboard (OB) blanket module (d) are shown. The model is a 3D *quasi*-heterogenized design in which most of the details are included and with the equatorial OB module fully heterogenized (stiffening plates, flow channel inserts (FCI), breeder channels, walls are all separately described).

The chemical compositions for all the materials include relevant impurities because often they give rise to significant additional activation compared to the base material. The compositions considered for Eurofer, W, PbLi, are given in [14][15] and [16] respectively and summarized in Table 1, while SS-316L(N)-IG austenitic steel have been used for VV and out-vessel steel components. The lead-lithium breeder material (with 90% enrichment in ^{6}Li) has been considered motionless for the purpose of this study notwithstanding it actually flows through the breeding regions with a velocity of about 0.2 m/s. This is a conservative assumption since the time of exposure to radiation is overestimated.

In original neutronics model the divertor is modelled as a full solid steel body of Eurofer97 except two layers facing the plasma of 5 mm thick tungsten armour, with in between a 15 mm thick tube layer filled with a homogenized mixture of 39.5% W, 17% CuCrZr, 13% Cu and 30% water. Another composition has been also tested substituting the massive steel box for a cassette made by 54%$_{vol}$ Eurofer and 46%$_{vol}$ water with reduced density of 2.43 g/cm^3 (also equivalent to 28.3%$_{vol}$ Eurofer, 24%$_{vol}$ water and rest (47.7%$_{vol}$) void) as according to the 2015 divertor design [17][18].

The reactor fusion power is 2037 MW corresponding to 7.323×10^{20} n/s source, with an average neutron wall loading of 1.032 MW/m^2. The plasma parameters (radios, elongation, triangularity, radial shift, and source peaking factor) correspond to those of DEMO baseline 2015 design [10]. The neutron source is described by a parametric representation of typical fusion L-mode confined plasma using an external subroutine and applied using proper parameters inside the MCNP input [11].

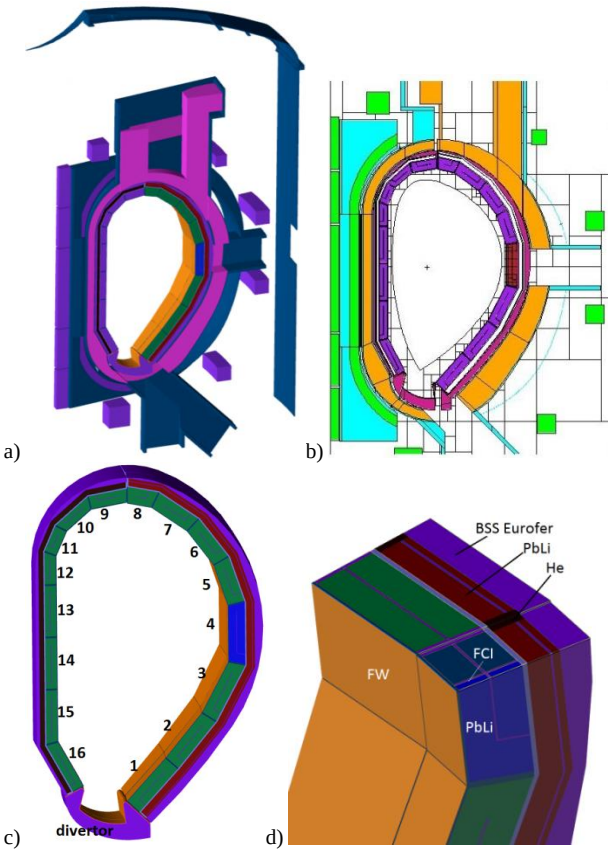

Figure 1. DCLL DEMO2015: a) whole reactor; b) MCNP geometry plot; c) BB segment, BSS and divertor; d) detail of OB BB module (partially heterogenized) and its fully-heterogenized BSS, version 3.0

The radiation transport calculations have been performed using Monte Carlo code MCNP5 and JEFF3.2 [19] cross section data library. The activation responses have been then determined by the use of the inventory code ACAB and the nuclear data library EAF2007 [20]. The activation calculations have been performed on CIEMAT EULER cluster, while the Advanced D1S shutdown dose rate calculations have been performed on ENEA HPC CRESCO cluster using 256 processors/run with $1x10^9$ neutron particles.

Table1. Isotopic compositions for Eurofer, PbLi and W

	Weight %		
Isotope	**Eurofer**	**PbLi**	**W**
H	-	-	0.0005
Li	-	0.62	-
B	0.001	-	-
C	0.105	-	0.003
N	0.04	-	0.0005
O	0.001	-	0.002
Na	-	-	0.001
Mg	-	-	0.0005
Al	0.004	0.01	0.002
Si	0.026	0.01	0.002
P	0.002	-	0.002
S	0.003	-	0.0005
K	-	-	0.001
Ca	-	-	0.0005
Ti	0.001	-	0.0005
V	0.2	0.005	-
Cr	9	0.005	0.002
Mn	0.55	0.005	0.0005
Fe	88.821	0.005	0.003
Co	0.005	-	0.001
Ni	0.01	0.005	0.0005
Cu	0.003	0.001	0.001
Zn	-	0.001	0.0005
As	-	-	0.0005
Zr	-	-	0.0005
Nb	0.005	0.001	0.001
Mo	0.003	0.005	0.010
Pd	-	0.001	-
Ag	-	0.001	0.001
Cd	-	-	0.0005
Sn	-	0.02	-
Ba	-	-	0.0005
Ta	0.12	-	0.002
W	1.1	0.02	99.96
Pb	-	99.265	0.0005
Bi	-	0.02	-

2.3 Calculation of temporal correction factors

The irradiation scenario assumed for the activation calculations is based on the operation scheme specified for the 1st DEMO phase [21]: continuous operation over 5.2 years (CY) minus 10 days at 30% of the nominal fusion power followed by 10 days pulsed operation with 48 pulses of 4 hours at full power and 1 hour dwell time in between, reaching a total of 1.57 FPY. Even if the divertor could be replaced once during this time in the present simulations the replacement of the components was disregarded. This means that all the structures are exposed to the neutron irradiation during the same lifetime.

The decay times considered for the results are: 1 day, 12 days and 1 year.

The time correction factors are calculated in an initial phase with an inventory code and they are stored in a proper text file which is read by Advanced D1S modified MCNP during the coupled n-decay γ simulation. Such temporal correction factors calculated with FISPACT inventory code [7] in earlier DEMO applications [22][23], have been now calculated with ACAB [8] at those different cooling times (see Table 2). The comparison of ACAB with FISPACT values at 12 days are also shown in Table 2 with the corresponding ACAB/FISPACT ratio. The temporal correction factors provided by both codes are in optimal agreement, providing validation of the implementation strategy of the approach on ACAB code as well. To compute such correction factors two ACAB inputs need to be run: one considering the real irradiation DEMO history described above, and the second with the whole irradiation history condensed in one second. The two inputs have to consider the same spectra, in our case the First Wall (FW) of the OB equatorial module.

For this calculation the material used is a fictitious material created *ad-hoc* according to the specific application containing all the major parent nuclides of the most important activation products foreseen. In our cases the fictitious material contains: F, Mg, Al, Si, Cr, Mn, Fe, Co, Cu, Nb, Mo, Ag, Ta and W.

The time correction factor for the *k*-nuclide is the ratio between the *k*-activities at the cooling time t_{cool} (1st ACAB run) and the total number of *k*-nuclides produced at the end of a fictitious instantaneous irradiation (T_{irr}= 1 s) [5], i.e. assuming that all the neutrons (total neutron yield, $Y_n = \int_0^{T_{irr}} \frac{dn}{dt'} dt'$) are emitted in one second (2nd ACAB run):

$$\tau_k^{-1}(t)|t_{cool} = \frac{A_k\,(t)|t_{cool}}{N_k|T_{irr} = 1s, t_{cool} \to 0}$$

where: $A_k(t)|t_{cool}$ is the activity of *k*-radionuclide at t = t_{cool} and $N_k|T_{irr}=1s,t_{cool}\to 0$ is the number of atoms of *k*-radionuclide at the end of instantaneous irradiation. As the total irradiation time is $1.639x10^8$ s, the neutron yield for the $7.323e^{20}$ n/s yield rate is $1.185x10^{29}$ n.

Except for multistep reactions and isomeric transitions the correction factor is independent from the neutron spectrum, activation cross section and amount of parent nuclides. It depends only on the irradiation history [5].

Then, the different contributions to the dose rate multiplied by the proper time correction factor and the total neutron yield are summed to obtain the total shutdown dose rate which is:

$$\dot{D}(t)|t_{cool} = 3.6 \times 10^{-3} \cdot Y_n \sum_k D_k|_{MCNP} \cdot \tau_k^{-1}(t)$$

where the numerical factor 3.6 x 10^{-3} is applied to convert the pSv/s to μSv/h.

On the basis of preliminary evaluations and past experiences [22] only a limited number of reactions have been considered for activation. At 12 days after shutdown, gammas from the decay of Co-58, Co-60, Mn-54, Ta-182 and Fe-59 were identified as the dominant contributors to the doses. Many others have been considered at 1 day because of the major number of short-live nuclides contributing substantially to the activation responses. The reactions considered at the three cooling times considered are shown in Table 3. It should be noted that there are not W activation reactions because cross-sections of W activation and decay gamma production are not presently available in the Advanced D1S modified format. Activation pre-analyses performed with MCNP5 and FISPACT showed [22] that the lack of W activation is important at short cooling times. Indeed, at 1 day after shutdown the contact dose rate of W is slightly higher than Eurofer in plasma facing components. At longer cooling times the contact dose in W was a factor ~7 and two orders of magnitude less than contact dose in Eurofer at 12 days and 1 year after shutdown, respectively. Then an underestimation in divertor region is expected due to the lack of W activation of plasma facing component mainly at 1 day after shutdown.

Table 2: Correction factors calculated with ACAB for the main activation products at 1 day, 12 days and 1 year since shutdown. Comparison with FISPACT values at 12 days are also shown with the corresponding ACAB/FISPACT ratio.

	Time after shutdown (sec)				
Daughter nuclide	1day ACAB	12days ACAB	12days FISPACT	ratio A/F_{12d}	1year ACAB
Mn54	7.96E+11	7.77E+11	7.78E+11	0.998	3.55E+11
Mn56	3.69E+09				
Co57	8.45E+11				
Co58g+m	8.94E+11	8.03E+11	8.18E+11	0.982	2.54E+10
Co60g+m	3.91E+11	3.89E+11	3.88E+11	1.003	3.43E+11
Ni57	1.31E+12				
Ni65	3.20E+09				
Cu64	5.76E+11	3.18E+05	3.35E+05	0.949	
Cr51	1.04E+12	7.92E+11	7.99E+11	0.992	1.16E+08
Nb91	5.32E+09				
Nb92m	1.34E+12				
Nb94	4.50E+08	4.50E+08	4.56E+08	0.987	4.50E+08
Nb95	3.01E+12				
Mo99	1.54E+12				
Tc99	9.01E+12				
Ag106m	1.37E+12				
Ag110m	8.00E+11				
Ta182	8.45E+11	7.90E+11	8.09E+11	0.977	9.36E+10
Na24	7.00E+11				
Fe55	5.81E+11	5.76E+11	5.76E+11	1.000	4.51E+11
Fe59	9.58E+11	8.07E+11	8.15E+11	0.990	3.30E+09

Table 3: Selected activation reactions

Parent Isotope	Reaction	Daughter	1 day	12 day	1 year
		Isotope			
^{55}Mn	(n,2n)	^{54}Mn	x	x	x
^{55}Mn	(n,γ)	^{56}Mn	x		
^{54}Fe	(n,p)	^{54}Mn	x	x	x
^{56}Fe	(n,2n)	^{55}Fe	x	x	x
^{50}Cr	(n,γ)	^{51}Cr	x	x	x
^{52}Cr	(n,2n)	^{51}Cr	x	x	x
^{58}Fe	(n,γ)	^{59}Fe	x	x	x
^{58}Ni	(n,p)	^{58}Co	x	x	x
^{58}Ni	(n,2n)	^{57}Ni	x	x	x
^{60}Ni	(n,p)	^{60}Co	x	x	x
^{61}Ni	(n,p)	^{61}Co	x		
^{61}Ni	(n,np)	^{60}Co	x	x	x
^{62}Ni	(n,p)	^{62}Co	x		
^{62}Ni	(n,np)	^{61}Co	x		
^{64}Ni	(n,γ)	^{65}Ni	x		
^{59}Co	(n,γ)	^{60}Co	x	x	x
^{59}Co	(n,2n)	^{58}Co	x	x	x
^{65}Cu	(n,2n)	^{64}Cu	x	x	x
^{65}Cu	(n,p)	^{65}Ni	x	x	x
^{65}Cu	(n,α)	^{62}Co	x	x	x
^{63}Cu	(n,α)	^{60}Co	x	x	x
^{63}Cu	(n,γ)	^{64}Cu	x	x	x
^{63}Cu	(n,2n)	^{62}Cu	x	x	x
^{93}Nb	(n,γ)	^{94}Nb	x	x	x
^{93}Nb	(n,2n)	^{92}Nb	x	x	x
^{181}Ta	(n,γ)	^{182}Ta	x	x	x
^{92}Mo	(n,np)	^{91}Nb	x		
^{95}Mo	(n,p)	^{95}Nb	x		
^{96}Mo	(n,np)	^{95}Nb	x		

Lastly, in order to calculate the shutdown doses the fluence-to-Effective dose conversion coefficients taken from ICRP 74 have been applied [24] (Table 4).

Table 4: Conversion coefficients gamma flux (Φ)-to-dose (E)

photon energy, MeV	E/Φ pSv•cm^2
0.010	0.0485
0.015	0.1254
0.02	0.2050
0.03	0.2999
0.04	0.3381
0.05	0.3572
0.06	0.3780
0.07	0.4066
0.08	0.4399
0.10	0.5172
0.15	0.7523
0.2	1.0041
0.3	1.5083
0.4	1.9958
0.5	2.4657
0.6	2.9082
0.8	3.7269
1	4.4834
2	7.4896
4	12.015
6	15.987
8	19.919
10	23.760

3-D maps in the whole reactor for the shutdown dose rates, the decay gamma fluxes and decay gamma heating for Eurofer structures have been then provided using the MESH tally capability of MCNP5 with the Advanced D1S code, and specific values at some relevant positions have been calculated as well (cell-

based F4 tallies). These are spherical void cells located inside the vessel in front of the inboard (IB) equatorial module (1), behind the OB equatorial module (2), on the bottom close to the divertor (3) and on the top (4). Such positions are shown in Figure 2.

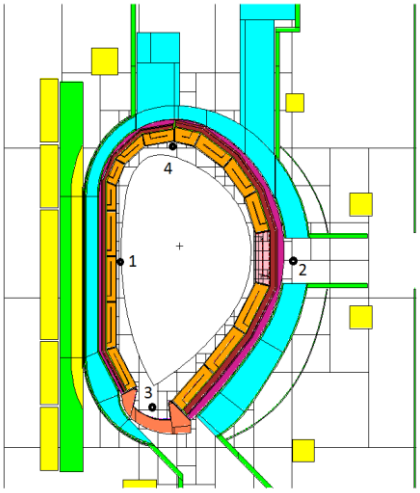

Figure 2. MCNP DCLL DEMO model with the 4 detector in which the responses have been calculated as local values.

The responses have been provided at 1, 12 days and 1 year after shutdown and for two DCLL DEMO models having different divertor compositions. For the local values at the 4 positions of interest the contribution of each radionuclide to the dose rate has also been separately provided.

3. Results

3.1 Results at 12 days after shutdown

First of all, the results have been analysed at the relevant time of 12 days after shutdown, since this time is used to plan the area classification and the access limitation for the maintenance activities in ITER [25].

3D maps results have been produced by means of the FMESH tally feature using a mesh made of 32x20x25 cm^3 voxels for decay heat and decay flux and a higher spatial resolution with 16x10x12.5 cm^3 voxels for the shutdown dose rate maps.

The SDR map is shown in Figure 3 giving results for the two different divertor models. The statistical error is very good, within 5% in all the zones of interest as shown in Figure 4 (obtained in 18 hours run). The range for the entire reactor goes approximately from 2000 to 0.01 Sv/h when adopting the full Eurofer cassette divertor while the SDR overpass this scale (using for such values a deep-purple colour) in punctual divertor zones when the 2015 divertor composition is used. The 3D map shows an extremely high difference between the IB and OB BSS values being around 5 Sv/h in the OB equatorial region and 50 Sv/h in the IB one implying a factor 10 of difference.

According to the specific detector values given in Table 5, the maximum SDR at 12 days after the shutdown results ≈1350 Sv/h in the Bottom (3) zone when the 2015 divertor composition is used. At the OB equatorial port (2), the maximum value is ≈15 Sv/h while ~1000 Sv/h is the maximum in the IB equatorial (1) and Top (4) in-vessel positions.

The table shows also the different contribution to the total SDR for the most important radionuclides at12 days after shutdown.

A selection of the major nuclides which contribution is higher than 1 Sv/h is also plotted in Figure 5. The major contribution to the SDR in position 1 (IB equatorial), 3 (Bottom) and 4 (Top) is due to Mn-54 ($T_{1/2}$ ~312 days) and Ta-182 ($T_{1/2}$ ~115 days) decay. The Mn-54 is generated mainly from Fe-54 (n,p) and Mn-55 (n,2n) reactions. With the current AD1S library, the Ta-182 is generated only by Ta-181 (n,γ) and it might be underestimated because the reaction W182(n,2n)W181(b+)Ta181(n,γ)Ta182 is missing and it might imply an underestimation of few % especially close to the FW and to the divertor. In OB position (2) the contribution of the Tantalum dominates (~59%). This is due to the low-energy neutrons slowed down through blanket-BSS in the equatorial port region. Co-60 ($T_{1/2}$ ~5.3 years) is also a main contributor in such position (~35%). Fe-59 ($T_{1/2}$ ~44.5 days) is also contributing in the three inner positions (1, 3 and 4) and Co-58 ($T_{1/2}$ ~70.9 days) in position 1 although in much reduced amount.

The use of a different divertor composition is reflected in the result of the SDR in position 3 (Bottom): 570 vs. 1350 Sv/h are the results by using the normal steel divertor vs. the improved water cooled steel divertor. In the first case the contributors to dose are mainly Mn54 (63%) and Ta182 (32%) while in the second case besides Ta182 (40%) and Mn54 (25%) appears Co60 ($T_{1/2}$ ~5.27 years) contributing a 32%. The differences in Co60 due to the divertor are also highlighted in Figure 6 which show the total fluxes and the specific contribution of Co60 for both divertor compositions and in position 1 (Figure 6a) and 3 (Figure 6b), respectively. The profiles indicate that the divertor composition influences mainly but not only its surroundings but also the proximity of the IB eq. zone. The use of water coolant in the divertor implies the increase of the low energy component inside the entire plasma chamber, consequent increase of the neutron flux in the thermal region of the spectrum, higher neutron absorption in steel and higher photon emission causing activation. More details on the effect of divertor design on the radiation field inside the plasma chamber are described in [26].

Table 5. Left: Shutdown dose rate with contribution for the most relevant nuclides at 12 days after shutdown at the positions 1-4 and for the 2 different divertor compositions. Right: Decay gamma fluxes and heating for the 4 positions and the 2 types of divertor used.

Radioactive Isotope	1 - IB		2 - OB		3 - Bottom		4 - Top	
Co58	1.07E+00	0.10%	4.31E-02	0.27%	5.24E-01	0.09%	7.72E-01	0.08%
Co60	2.68E+00	0.25%	5.58E+00	**35.30%**	7.24E+00	1.27%	3.41E+00	0.34%
Fe59	1.40E+01	1.33%	7.24E-01	4.58%	1.46E+01	2.57%	1.48E+01	1.48%
Mn54	9.26E+02	**88.12%**	1.33E-01	0.84%	3.60E+02	**63.25%**	8.62E+02	**86.20%**
Ta182	1.07E+02	**10.20%**	9.33E+00	**59.01%**	1.87E+02	**32.82%**	1.19E+02	**11.90%**
total	1.05E+03	100%	1.58E+01	100%	5.70E+02	100%	1.00E+03	100%
	1 - IB Div2015		2 - OB Div2015		3 - Bottom Div2015		4– Top Div2015	
Co58	1.41E+00	0.13%	4.30E-02	0.28%	6.10E-01	0.05%	9.97E-01	0.10%
Co60	2.34E+01	2.14%	5.45E+00	**35.05%**	4.43E+02	**32.89%**	1.78E+01	1.70%
Fe59	1.36E+01	1.24%	7.07E-01	4.54%	2.84E+01	2.11%	1.45E+01	1.39%
Mn54	9.25E+02	**84.43%**	1.33E-01	0.86%	3.37E+02	**25.02%**	8.74E+02	**83.46%**
Ta182	1.32E+02	**12.06%**	9.22E+00	**59.28%**	5.38E+02	**39.94%**	1.40E+02	**13.36%**
total	1.10E+03	100%	1.56E+01	100%	1.35E+03	100%	1.05E+03	100%

	Decay gamma flux (γ/cm^2/s)	
pos	full Eurofer Divertor	2015 Divertor
1	9.00E+10	9.40E+10
2	1.43E+09	1.42E+09
3	4.66E+10	1.19E+11
4	8.58E+10	9.00E+10

	Decay Heat (W/cm^3)	
pos	full Eurofer Divertor	2015 Divertor
1	2.35E-03	2.45E-03
2	3.78E-05	3.72E-05
3	1.32E-03	3.06E-03
4	2.27E-03	2.35E-03

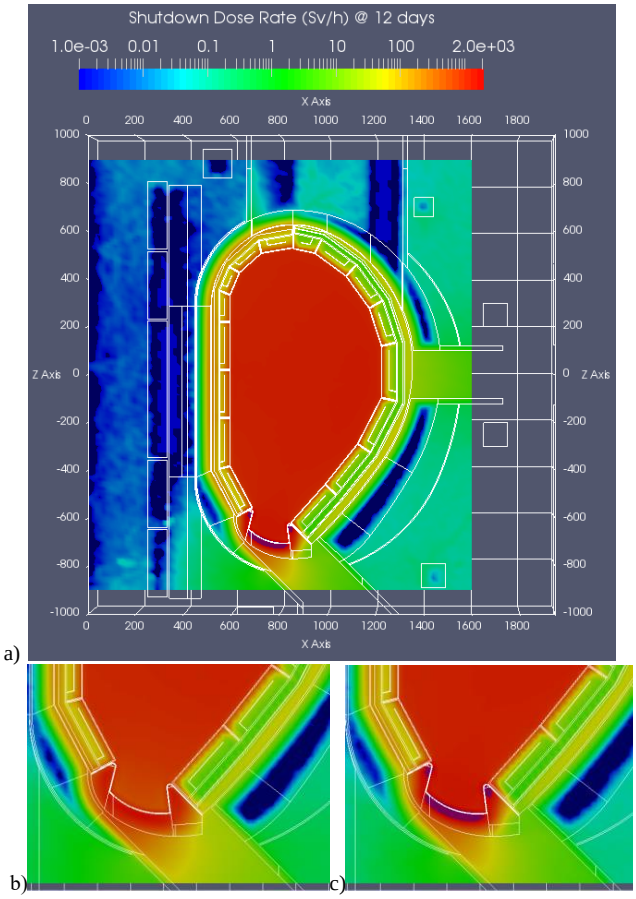

Figure 3: a) SDR 3D mesh tally map at 12 days after shutdown; comparison between the full-Eurofer (b) and the 2015 (c) divertor is also shown. Values outside the adopted scale are in deep-blue (under the scale) and deep-purple (over the scale) colours.

The total decay gamma fluxes are also given for the four detectors positions in Figure 7 and as 3D maps covering the entire reactor in Figure 8. The comparison given in Figure 7 shows strong differences in the profiles at position 3 with two peaks at 0.55 and 1.5 MeV not observed when the full-Eurofer divertor composition is used.

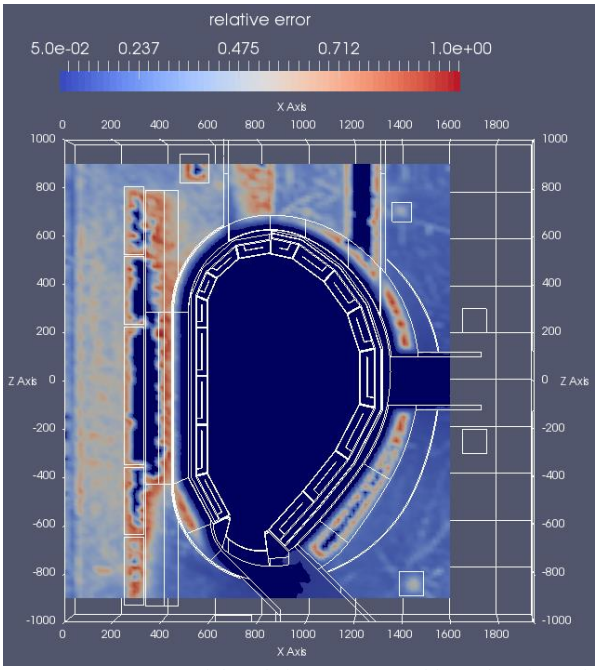

Figure 4: SDR 3D map of the relative error. Deep-blue colour is used for the values under the scale.

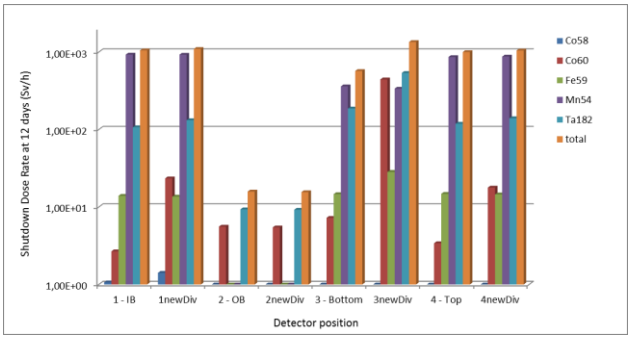

Figure 5: SDR contribution of dominant nuclides at 12 days since shutdown for the 2 divertor compositions and at 4 different locations.

According to the mesh results of Figure 8 and also to the specific values given in Table 5 (right-up) the decay gamma flux ranges between ≈4.7x10^{10} and ≈1.2x10^{11} γ/cm^2/s inside the vessel (around position 3) depending on the divertor considered and reaching a maximum of ≈3x10^{11} γ/cm^2/s right on the top of the divertor component when the 2015 composition with water is used. Inside the Equatorial and Lower Port the fluxes are higher than 10^9 γ/cm^2/s being 1.4x10^9 γ/cm^2/s the value in position 2 (OB equatorial on vessel). They slow down up to 3·10^8 γ/cm^2/s, at the end of the port behind the OB TF coil zone. The 3D map shows high difference between the IB and OB BSS values being around 3-4·10^9 in the OB equatorial region and 10^{10} in the IB one.

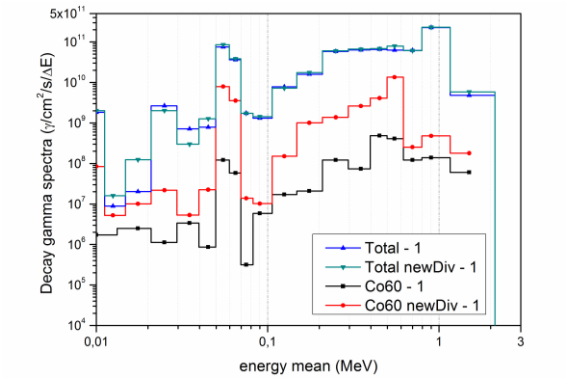

a)

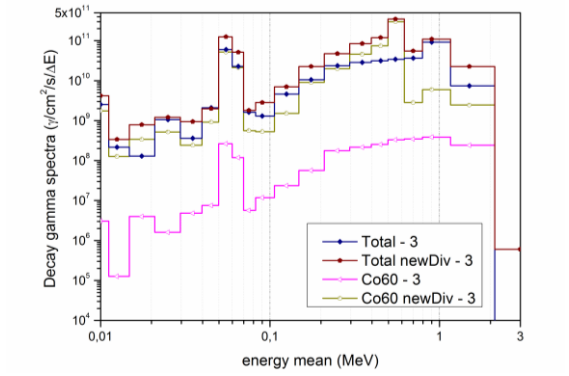

b)

Figure 6. Decay gamma spectra (γ/cm^2/s) in position #1(a) and #3 (b) with the specific Co60 contribution.

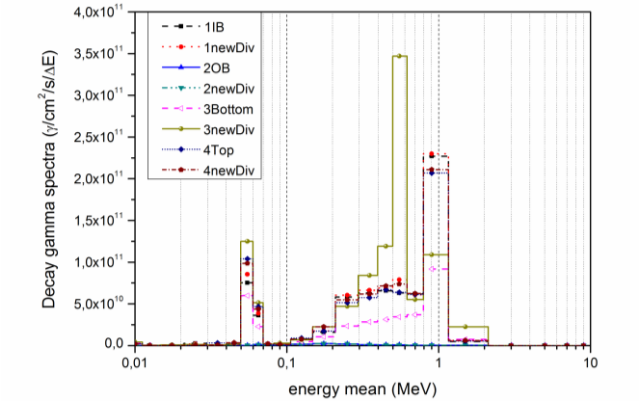

Figure 7. Decay gamma spectra (γ/cm^2/s) at the four detector positions at 12 days after shutdown.

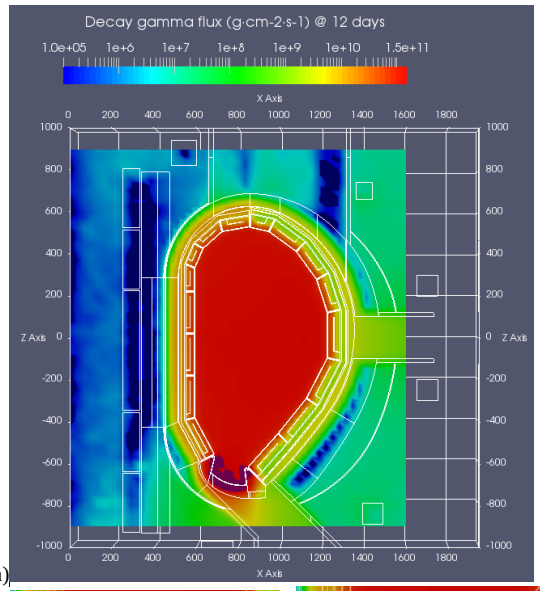

a)

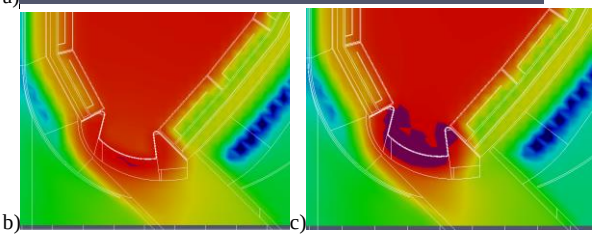

b) c)

Figure 8: a) Decay Gamma flux 3D map; comparison between the (b) full-Eurofer and (c) 2015 divertor. Values outside the adopted scale are in deep-blue and deep-purple colours.

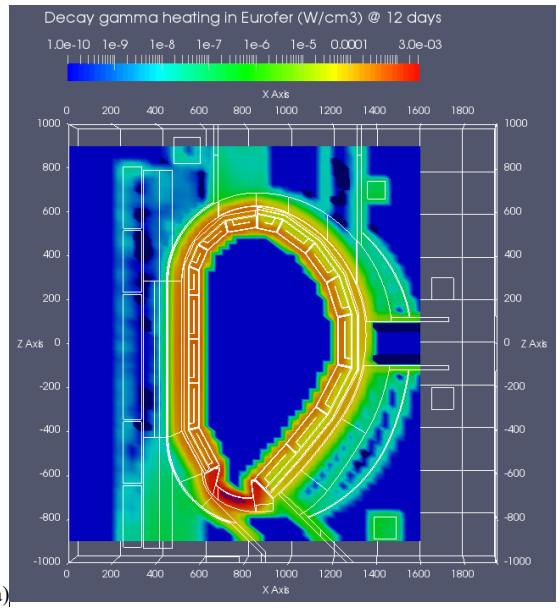

a)

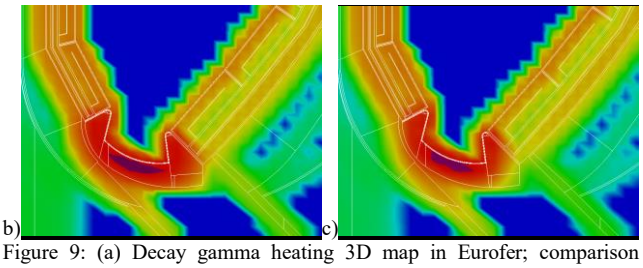

b) c)

Figure 9: (a) Decay gamma heating 3D map in Eurofer; comparison between the (b) full-Eurofer and (c) 2015 divertor. Values outside the adopted scale are in deep-blue and deep-purple colours.

The decay gamma heat on Eurofer components has been also calculated (Table 5 right-down). The decay heat is ≈1.3-3x10^{-3} W/cm^3 on the divertor detectors (position 3) for the old and new cassette and ≈2.5x10^{-3} on the FW detectors (position 1 and 4). The value obtained for a FW spectrum of the IB equatorial module using the direct ACAB estimation is 2.47x10^{-3} W/cm^3 in line with the 2.35–2.45x10^{-3} W/cm^3 obtained through the Advanced D1S method. According to the mesh tally 3D maps displayed in Figure 9, the differences among IB and OB in the Eurofer BSS behind the blankets are high, showing a factor 10 of difference.

3.2 Results at 1 day and 1 year after shutdown

Other two times of interest are at 1 day [25] and 1 year of cooling after the shutdown of the machine.

Activation analyses have been performed at this two cooling times although only for the DCLL DEMO model with the 2015 divertor composition.

Shutdown dose rate, decay gamma fluxes and decay gamma heating 3D maps at 1 day after shutdown are given in Figures 10 a, c, and e, respectively. Marginal differences with respect to the same 3-D maps at 12 days after shutdown are shown.

According to the specific detector values given in Table 6, the maximum SDR at 1 day after the shutdown results 1408 Sv/h in the Bottom (3) zone to be compared with 1350 Sv/h calculated at 12 days. At the OB equatorial port (2), the value is 16.88 Sv/h while 1168 and 1118 Sv/h are the results in the IB equatorial (1) and Top (4) zones to be compared respectively with the ~15.6, 1100 and 1050 Sv/h of (2), (1), and (4) at 12 days.

The major contribution to the SDR, as in the 12 days case, is due to Mn-54, Ta-182 and Co-60 decay (Figure 11). Mn-56 and Fe-59 contributes ~1-3% and Fe-59 reaches ~5% in OB-2 detector. Comparing the contributions greater than 1 Sv/h, as displayed in Figures 5 and 11 for the cases at 12 days and 1 day respectively, at 1 day Mn-56 ($T_{1/2}$ ~2.6 hours) and Cr-51 ($T_{1/2}$ ~27.7 days) are present while their contribution is negligible at 12 days. Comparing Tables 5 and 6 which show all the contributors to the SDR, Ni-65, Nb-94 and Co-62 are also present at 1 day - although in a reduced amount - while at 12 they were not considered among the activated reactions.

In general, the tabulated values of SDR (left Table 6), decay gamma fluxes (right-up Table 6) and decay gamma heating (right-down Table 6) at 1 day are very similar to the corresponding ones (Tables 5) at 12 days when the same divertor is used.

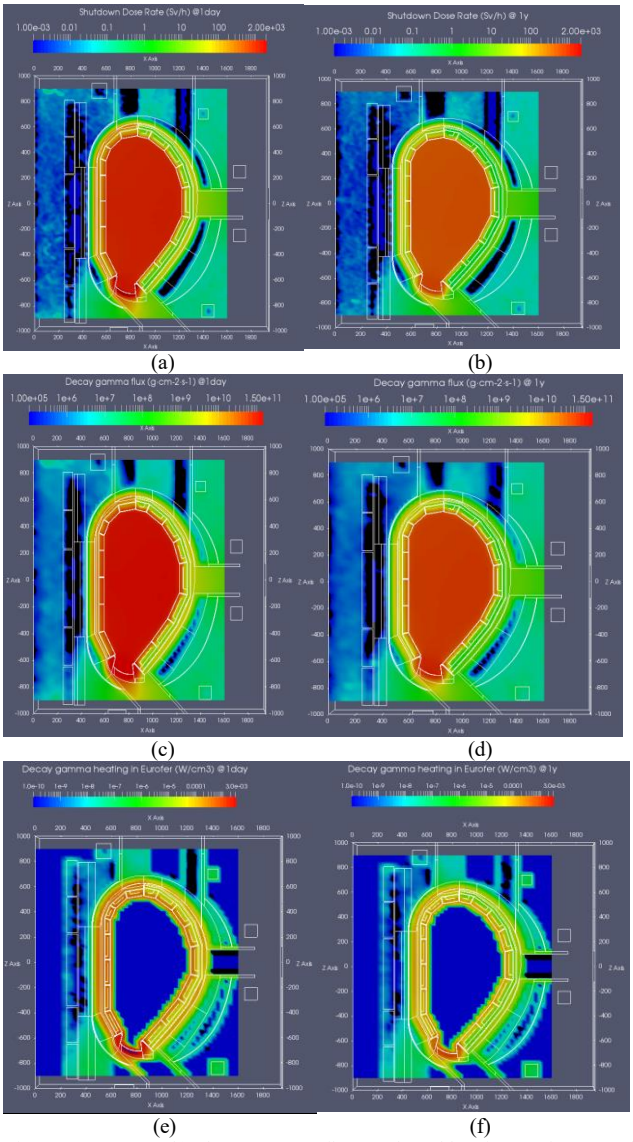

Figure 10: SDR (a, b), decay gamma flux (c, d) and heating (e, f) 3D mesh tally maps at 1 day (left) and 1 year (right) after shutdown. Values outside the adopted scale are in black and deep-purple colours.

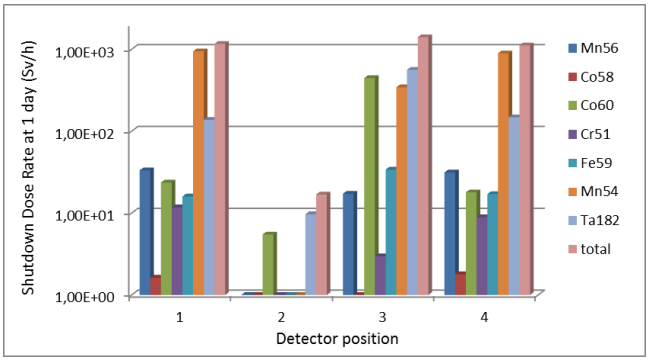

Figure 11: SDR contribution of dominant nuclides at 1 day after shutdown at the 4 different locations.

At 1 year after shutdown, comparing with the results obtained at 12 days (Tables 5), the SDR, decay gamma fluxes and decay gamma heating are reduced a factor between 1.9 and 2.65 in all the detector positions (see Tables 6). 3D maps for the three responses of interest are also given in Figures 10 b, d and f for comparison

with the previous ones. The dose rate at 1 year after shutdown is due mainly to three radionuclides: Mn-54, Co-60 and Ta-182 (Figure 12).

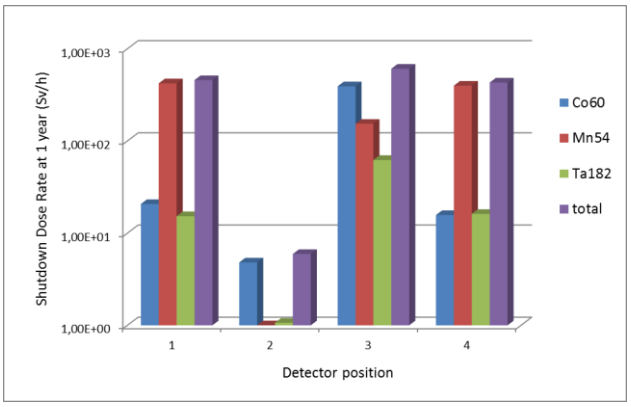

Figure 12: SDR contribution of dominant nuclides at 1 year after shutdown at the 4 different locations.

According to Table 6 and Figure 12, Mn-54 is the dominant nuclide in position 1 and 4, and comparing with the previous results at 12 day its contribution passes from 84% to 92% while the Ta-182 contribution drops from 12% to 3%. Co-60 has now an extremely high contribution both in position 2 (passing from 35% to 80%) and 3 (from 32% to 64%) at the expense of Ta-182 and Mn-54. As shown in Figure 12 they are practically not more displayed in position 2.

Table 6. Left: Shutdown dose rate with contribution for the most relevant nuclides at 1 day and 1year after shutdown at the positions 1-4. Right: Decay gamma fluxes and heating for the 4 positions for 1 day and 1 year after shutdown.

1 day								
Radioactive Isotope	1 - IB	contrib to TOT	2 - OB	contrib to TOT	3 - Bottom	contrib to TOT	4 - Top	contrib to TOT
Mn56	3.33E+01	2.85%	3.60E-01	2.13%	1.72E+01	1.22%	3.14E+01	2.81%
Co58	1.63E+00	0.14%	1.07E-01	0.63%	6.66E-01	0.05%	1.80E+00	0.16%
Ni65	8.69E-06	0.00%	4.64E-04	0.00%	4.97E-06	0.00%	8.70E-06	0.00%
Co60	2.36E+01	2.02%	5.49E+00	**32.54%**	4.46E+02	**31.68%**	1.79E+01	1.60%
Cr51	1.18E+01	1.01%	2.52E-01	1.49%	2.98E+00	0.21%	8.93E+00	0.80%
Co62	1.24E-11	0.00%	8.23E-15	0.00%	2.47E-10	0.00%	9.01E-12	0.00%
Nb94	6.73E-04	0.00%	2.63E-05	0.00%	3.74E-04	0.00%	6.96E-04	0.00%
Fe59	1.60E+01	1.37%	8.30E-01	4.92%	3.40E+01	2.41%	1.71E+01	1.53%
Mn54	9.46E+02	**80.98%**	1.36E-01	0.81%	3.45E+02	**24.47%**	8.93E+02	**79.89%**
Ta182	1.38E+02	**11.81%**	9.70E+00	**57.48%**	5.63E+02	**39.96%**	1.48E+02	**13.21%**
total	1.17E+03	100%	1.69E+01	100%	1.41E+03	100%	1.12E+03	100%

Decay gamma flux (γ/cm^2/s)		
pos	1 day	1year
1	1.01E+11	4.03E+10
2	1.60E+09	5.39E+08
3	1.23E+11	6.17E+10
4	9.65E+10	3.80E+10

Decay Heat (W/cm^3)		
pos	1 day	1year
1	2.65E-03	1.03E-03
2	4.13E-05	1.40E-05
3	3.24E-03	1.42E-03
4	2.53E-03	9.67E-04

1 year								
Radioactive Isotope	1 - IB	contrib to TOT	2 - OB	contrib to TOT	3 - Bottom	contrib to TOT	4 - Top	contrib to TOT
Co58	4.39E-02	0.01%	1.34E-03	0.02%	1.90E-02	0.00%	3.10E-02	0.01%
Co60	2.07E+01	4.52%	4.82E+00	**80.97%**	3.91E+02	**64.44%**	1.57E+01	**3.66%**
Fe59	5.50E-02	0.01%	2.86E-03	0.05%	1.15E-01	0.02%	5.88E-02	0.01%
Mn54	4.22E+02	**92.11%**	6.08E-02	1.02%	1.54E+02	**25.29%**	3.98E+02	**92.56%**
Ta182	1.53E+01	3.34%	1.07E+00	**17.94%**	6.23E+01	**10.25%**	1.62E+01	**3.76%**
total	4.58E+02	100%	5.95E+00	100%	6.07E+02	100%	4.30E+02	100%

4. General considerations on application of Advanced D1S to DCLL DEMO analyses

The Advanced D1S code applied on DEMO-DCLL showed optimal performance in terms of speed and high statistical accuracy that can be obtained in very short time. However, the most important limitations are related to the lack of W activation cross reactions and of important multi-step activation reactions that may cause an underestimation of the shutdown dose rate. These cause underestimation especially in the in-vessel bottom region, because tungsten armour is the major plasma facing component of divertor. Furthermore the present version of the code cannot manage multiple lifetime components. Current activities are focused on the development of approximate technique to treat the most important multi-step reactions as single activation reaction and in extending the code capability to handle multiple irradiation histories [27].

5. Conclusions

The evaluation of the activation responses after the shutdown of the reactor is a major issue, due to their relevance for the planning of the maintenance operations. The Advanced D1S method coupling the MCNP5 transport code with the ACAB activation code has been applied at this purpose to the assessment of the DCLL DEMO model baseline 2015. The shutdown dose rates, decay gamma fluxes and heating

have been assessed both as 3D maps in the whole reactor both as tabulated values in four relevant detector positions at 1 day, 12 days and 1 year after the shutdown, breaking down the contribution of the major nuclides. In general, Mn-54 and Ta-182 have been identified as the most important nuclides in the in-vessel positions 1, 3 and 4, while in the OB equatorial Port the Co-60 provides a great contribution. This is also true when a new divertor composition with major water content is used. From 1 day to 12 days the contribution from Mn-56, Ni-65 and Cr-51 results very reduced or almost disappears by decay. From 12 days to 1 year the responses drop to more than a half and the major contributors are Mn-54 and Co-60.

Acknowledgments

This work has been carried out within the framework of the EUROfusion Consortium and has received funding from the Euratom research and training programme 2014-2018 under grant agreement No 633053. The views and opinions expressed herein do not necessarily reflect those of the European Commission. The support from the EUROfusion Researcher Fellowship programme under the task agreement AWP15-ERG-CIEMAT/Palermo is gratefully acknowledged. The work has been partially supported by Spanish MINECO, HISMEFUS project ENE2013-43650-R, and by Comunidad de Madrid under TECHNOFUSION(II)-CM, S2013/MAE-2745.

The computing resources and the related technical support used for this work have been provided by CRESCO/ENEAGRID High Performance Computing infrastructure and its staff [28]. CRESCO/ENEAGRID High Performance Computing infrastructure is funded by ENEA, the Italian National Agency for New Technologies, Energy and Sustainable Economic Development and by Italian and European research programmes, see http://www.cresco.enea.it/english for information.

References

[1] Y. Chen, U. Fischer, MCNP based shutdown dose rate calculations: computational scheme, verification calculations and applications, Fusion Engineering and Design, 63-64 (2002), pp. 107–114.

[2] D. Valenza, H. Iida, R. Plenteda, R.T. Santoro, Proposal of shutdown estimation method by Monte Carlo code, Fusion Engineering and Design 55 (2001) 411–418.

[3] L. Petrizzi, H. Iida, D. Valenza, P. Batistoni, Improvement and benchmarking ofthe new shutdown dose estimation method by Monte Carlo code, in: Proc. ofthe Monte Carlo 2000 Conf., Lisboa, October 23-26, 2000, Springer, Berlin, 2001,pp. 865–870.

[4] R. Villari, P. Batistoni, S. Conroy, A. Manning, F. Moro, L. Petrizzi, et al., Shutdown dose rate benchmark experiment at JET to validate the three-dimensional Advanced-D1S method, Fusion Engineering and Design 87 (2012)1095–1100.

[5] R. Villari, U. Fischer, F. Moro, P. Pereslavtsev, L. Petrizzi, S. Podda, A. Serikov, Shutdown dose rate assessment with the Advanced D1S method: Development, applications and validation, Fusion Engineering and Design 89 (2014) 2083–2087

[6] X-5 Monte Carlo Team, "MCNP-A General Monte Carlo N-ParticleTransport Code: Version5 User's Guide", LANL report LA-CP-03-0245,2005.

[7] R. Forrest, FISPACT-2007 User Manual EASY 2007 Documentation Series UKAEA FUS 534.

[8] J. Sanz, O. Cabellos, N. Garria-Herranz, ACAB-2008, ACtivation ABacus Code V2008, NEA Data Bank (NEA-1839), 2009.

[9] Iole Palermo, David Rapisarda, Iván Fernández-Berceruelo, Angel Ibarra, Optimization process for the design of the DCLL blanket for the European DEMOnstration fusion reactor according to its nuclear performances (Nuclear Fusion (2017) 57 076011)

[10] Wenninger R., DEMO1 Reference Design - "EU DEMO1 2015" https://idm.euro-fusion.org/?uid=2LBJRY

[11] Pereslavtsev P., 2015 Generic DEMO Model for MCNP, https://idm.euro-fusion.org/?uid=2L6HJ7

[12] Wu Y. and F.D.S. Team 2009 CAD-based interface programs for fusion neutron transport simulation, Fusion Eng. Des. 84 1987–92

[13] Rapisarda D. *et al*, Conceptual Design of the EU-DEMO Dual Coolant Lithium Lead Equatorial Module, Transactions On Plasma Science http://dx.doi.org/10.1109/TPS.2016.2561204

[14] Final Report on the EFDA Article 7 contract EFDA/06-1903 on "Procurement of reduced activation ferritic-martensitic steel type 9CrWTaV (EUROFER) for the TBM fabrication technology trials and mock-ups", Saarschmiede GmbH, July 2009

[15] "Tungsten. Material properties and applications", PLANSEE SE, Reutte, Austria (2007), see www.plansee.com

[16] Technical specification for the EFDA Article 7 contract EFDA/05-998 on "Procurement of the Pb-Li eutectic alloy for EBBTF facility and for dedicated neutronics experiment", November 2009

[17] R. Villari., Neutronic Analysis Report for Divertor Cassette and PFC 2015, EFDA_D_2MN2H3 v1.0 June 2016

[18] J.H. You, Progress in the initial design activities for the European DEMO divertor: Subproject 'Cassette', Fus. Eng. Des. https://doi.org/10.1016/j.fusengdes.2017.03.018

[19] The JEFF-3.2 Nuclear Data Library, http://www.oecd-nea.org/dbforms/data/eva/evatapes/jeff_32/ NUCLEAR ENERGY AGENCY, OECD.

[20] R.A. Forrest, J. Kopecky, J.-Ch. Sublet, The European Activation File: EAF-2007 neutron-induced cross section library, UKAEA FUS 535, March 2007.

[21] J. Harman, WP12 DEMO Operational Concept Description, https://idm.euro-fusion.org/?uid=2LCY7A EFDA 2LCY7A 2012

[22] R. Villari, WPSAE_2.25.2-01, Status of D1S method development EFDA_D_2LHTFZ (2015).

[23] R. Villari, Status of D1S development- Final Report SAE-2.25.2-02 EFDA_D_2M86P5 (2016).

[24] ICRP publication 74, Conversion Coefficients for Use in Radiological Protection,Annals of ICRP 26/3, 1997.

[25] H. Iida, V. Khripunov, L. Petrizzi, G. Federici. Nuclear Analysis Report (NAR). ITER IDM location https://user.iter.org/?uid=22F2ST (2004).

[26] I. Palermo, R. Villari, A. Ibarra, Divertor options influence on DEMO nuclear performances, submitted to Fus. Eng. Des.

[27] R. Villari, et. al, Development of the Advanced D1S for shutdown dose rate calculations in fusion reactors, submitted to ANS transactions.

[28] G. Ponti et al., "The role of medium size facilities in the HPC ecosystem: the case of the new CRESCO4 cluster integrated in the ENEAGRID infrastructure", Proceedings of the 2014 International Conference on High Performance Computing and Simulation, HPCS 2014, art. no. 6903807, 1030-1033.